vehicles

MDPI

Article

Development of the Electrical Assistance System for a Modular Attachment Demonstrator Integrated in Lightweight Cycles Used for Urban Parcel Transportation

Vlad Teodorascu [1,2,*], Nicolae Burnete [1,2], Levente Botond Kocsis [1,2], Irina Duma [1,2], Nicolae Vlad Burnete [1,2], Andreia Molea [1,2] and Ioana Cristina Sechel [1,2]

[1] Department of Automotive Engineering and Transports, Technical University of Cluj-Napoca, 400641 Cluj-Napoca, Romania; nicolae.burnete@auto.utcluj.ro (N.B.); levente.kocsis@auto.utcluj.ro (L.B.K.); irina.duma@auto.utcluj.ro (I.D.); vlad.burnete@campus.utcluj.ro (N.V.B.); andreia.molea@auto.utcluj.ro (A.M.); ioana.sechel@auto.utcluj.ro (I.C.S.)
[2] European University of Technology, European Union
* Correspondence: vlad.teodorascu@campus.utcluj.ro

Abstract

A promising approach to advancing sustainable urban mobility is the increased use of light electric vehicles, such as e-cycles and their cargo-carrying variants: e-cargo cycles. These micromobility vehicles fall between e-cycles and conventional vehicles in terms of transport capacity, range, and cost. A key advantage of e-cargo cycles over their non-electrified counterparts is the electric powertrain, which enables them to carry heavier payloads, travel longer distances, and reduce driver fatigue. Since the primary use of e-cargo cycles is urban parchment deliveries, trip efficiency plays a critical role in their effectiveness within urban logistics. This efficiency is influenced by factors such as travel distance, traffic density, and the weight and volume of the delivery payload. While higher delivery capacity generally enhances efficiency, studies have shown that as the drop size increases, the efficiency of e-cargo cycle delivery trips tends to decline. A practical way to address this limitation is the use of cargo attachments, such as trailers. These micromobility solutions are already widely implemented globally and significantly enhance transport capacity. This paper reports the process of designing and testing the control algorithm of an electrical system for an experimental attachment demonstrator that can be used to convert most cycle vehicles into cargo variants. The system integrates two 250 W BLDC hub motors, two 576 Wh lithium-ion batteries, dual load-cell sensing in the coupling element, and an STM32-based controller to provide independent propulsion and synchronization with the leading cycle. The force-based control strategy enables automatic adaptation to varying payloads typically encountered in urban logistics, which is supported by the variable storage volume capable of transporting payloads of up to 200 kg.

Keywords: green logistics; smart cities; micromobility; sustainability; green mobility; cargo cycles

check for updates

Academic Editor: Mohammed Chadli

Received: 7 October 2025
Revised: 8 December 2025
Accepted: 11 December 2025
Published: 17 December 2025

Citation: Teodorascu, V.; Burnete, N.; Kocsis, L.B.; Duma, I.; Burnete, N.V.; Molea, A.; Sechel, I.C. Development of the Electrical Assistance System for a Modular Attachment Demonstrator Integrated in Lightweight Cycles Used for Urban Parcel Transportation. *Vehicles* **2025**, *7*, 164. https://doi.org/10.3390/vehicles7040164

Copyright: © 2025 by the authors. Licensee MDPI, Basel, Switzerland. This article is an open access article distributed under the terms and conditions of the Creative Commons Attribution (CC BY) license (https://creativecommons.org/licenses/by/4.0/).

1. Introduction

Green logistics initiatives in urban areas have increased the demand for electric vehicles, e-cargo bikes, and other e-mobility options as cleaner transportation alternatives. This shift has also heightened the demand for freight and passenger transport solutions capable

of operating effectively within the limited spaces of urban environments where micromobility solutions play a key role. This growing focus is reflected in multiple European projects and policy frameworks that promote micromobility and sustainable urban logistics. In the European Commission's "Sustainable and Smart Mobility Strategy" under the European Green Deal, an action plan with 82 measures to cut emissions by ~90% by 2050 is presented. Amongst these measures, multimodality is mentioned as a way to integrate micromobility with public transport solutions [1]. The "Fit for 55" package mandates zero-emission for all new cars by 2035 and with the wider Sustainable and Smart Mobility Strategy (SSMS), under the broader European Green Deal, which explicitly encourages, through active mobility funding investments, modal shift, multimodality and sustainable urban mobility solutions [2]. Other specific EU funded initiatives include "CityChangerCargoBike" which aims to accelerate cargo bike adoption in urban areas [3] and "ULaaDS", a project that emphasizes the benefits of light electric vehicles and e-cargo bikes when integrated into flexible, on-demand urban logistics systems [4].

Across numerous regions, cycle attachments and trailers are commonly employed to expand the transport capacity of bicycle-based systems in situations where alternatives are less economically viable [5]. Compared to a regular pedal electric cycle (PEDELEC) vehicle, trailers increase the transport capacity up to a factor of three, supporting payloads of up to 200 kg [6–8]. Other electrically assisted trailer solutions (eTrailers) available on the market leverage the advantages of the added modularity both for personal and business purposes. Performance specifications for four commercially available eTrailer models are shown in Table 1.

Table 1. Performance specifications for eTrailer products [9–11].

Manufacturer	Carla Cargo (Herbolzheim, Germany)	Aveon (Lormont, France)		NÜWIEL (Hamburg, Germany)
Product	**eCARLA**	**e-STD100**	**CARGO100**	**NÜWIEL**
Electric motor power [W]	250	≤1000 peak	≤1000 peak	250
Battery capacity [Wh]	720	optional	NR	600–800
Maximum allowed payload [kg]	200	45	100	150
Cargo volume [m^3]	1.5	0.16	NR	1
Top speed [km/h]	25	25	25	25

These products offer electrical assistance and easy integration with common cycle vehicles to enable the transportation of higher payloads although having fixed cargo volumes. Products such as eCARLA and NÜWIEL can also be used in a handheld mode, thus giving the option of large parcel manipulation over short distances [9,11].

Given the rising interest in micromobility as a means for reaching green transportation goals, this effort describes the development and testing of the electrical assistance system for a modular cargo attachment for cycles.

The attachment enables the use of most two-wheeled pedal vehicles for logistics purposes, providing increased versatility, reduced transport costs and energy use, and substantially lower greenhouse gas emissions and congestion compared with conventional delivery vehicles in dense urban areas.

2. Attachment Features

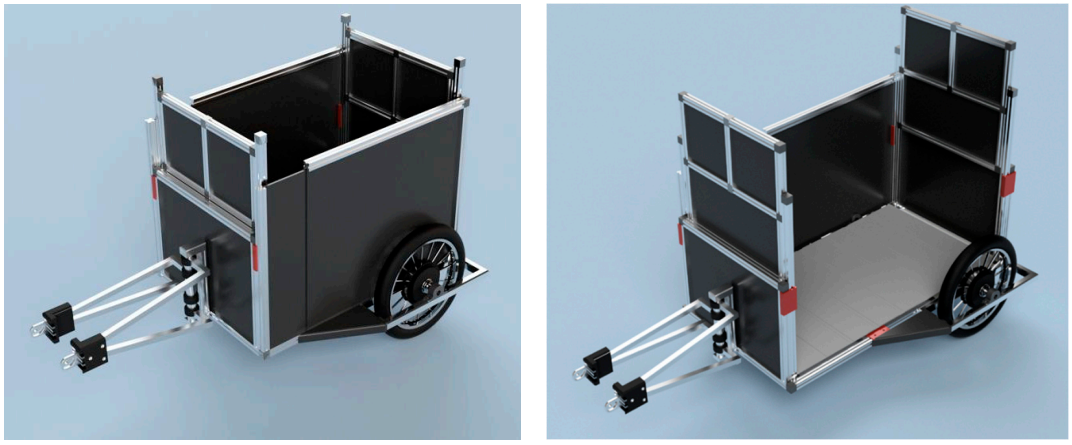
The development process of the attachment started with the requirements specification for the system. The present work precedes the fabrication of the attachment's mechanical structure. In [12], the development process of the three-dimensional CAD model is described, detailing the requirements for compliance with the legal framework as well as the safety standards incorporated into the design process. Furthermore, in [12] vehicle dynam-

ics simulations were performed using a mathematical model that identifies the stability conditions of the system and illustrated the various physical phenomena influencing its behavior. The simulations primarily examined parameters related to longitudinal stability, to analyze rollover tendency and wheel slip. The results revealed the limitations of the attachment through correlations between conditions such as road slope value, load mass, velocity and forces that act on the attachment's frame.

Compared to current pedal vehicle cargo transport options, the proposed solution introduces three features:

- Independent electric assistance: the attachment does not rely on the PEDELECs' electric assist system;
- Flexibility: the ability to adapt to various types of pedal vehicles through a universal coupling mechanism;
- Variable storage volume: to maximize transport efficiency [12].

An analysis of existing attachment and trailer designs [13–16] a three-dimensional model of the electrically assisted attachment was designed as shown in Figure 1.



(**a**) (**b**)

Figure 1. Three-dimensional renditions of the attachment: (**a**) Compact configuration; (**b**) Fully extended [12].

Two main characteristics of the system's design are its modularity and simplicity of the mechanical components that the users will interact with. Since the attachment integrates an electrical assistance system, the weight of its battery, motors, and wiring must be taken into account in the overall mass of the demonstrator. As a result, the materials chosen for the frame of the attachment must provide high durability, low weight, water resistance and sustainability [12].

Since the attachment is designed for urban logistics applications, particularly parcel and product delivery adherence to safety regulations and standardized vehicle dimensions is essential. Consequently, both the attachment and the cycle must comply with public road regulations meant for PEDELEC operation, including constraints on size, shape, and performance. Additionally, the adjustable cargo volume requires that all dimensional configurations comply with the relevant road-use regulations [17–20].

2.1. Hardware Characteristics

This research effort seeks to contribute to the decarbonization of urban transport by developing a modular electrically assisted attachment for pedal vehicles. Using an attachment for parcel transportation is an emerging application, as these systems are most

commonly used for transporting children. Since the system must be compatible with a wide range of cycle models, its functionality is defined by the following key requirements:

- The attachment must match the speed of the coupled cycle without disrupting natural pedaling dynamics or introducing excessive drag. This ensures a smooth riding experience while maintaining the natural dynamics of pedaling.
- The attachment should be capable of providing additional propulsion when necessary, such as during uphill climbs, rapid accelerations, or when extra assistance is needed due to rider fatigue.

The proposed solution aims to match the leading cycle's velocity by keeping the forces in the coupling mechanism as close to zero as possible. Thus, in the case of a positive resistive force, the trailer will accelerate so as not to increase the load on the leading vehicle, while in the case of a negative force, the trailer will brake to avoid pushing the leading vehicle during deceleration or stopping. By developing the control algorithm using a programmable microcontroller, the mentioned requirements are addressed through software functions.

To achieve full modularity, the attachment's propulsion system must be entirely independent and therefore must not rely on an external power source, such as an e-bike's battery system. Instead, it should incorporate an independent power supply that provides sufficient range and enables efficient energy management while ensuring adaptability across different cycle models. Dedicated sensors must be integrated to continuously gather essential data, including vehicle speed, applied torque, and real-time feedback from the electric motors. These sensors ensure optimal power delivery by adjusting motor output based on riding conditions and user input.

Given its intended functionality, the attachment's electrical architecture closely resembles that of an e-bike system, as it must fulfill similar operational requirements. The core components of the electrical assistance system include:

- A dedicated battery pack that supplies power to the system, designed to offer sufficient energy storage for extended use while maintaining a compact and lightweight profile.
- DC motors that provide the necessary propulsion characteristic, carefully selected based on power efficiency, torque output, and speed adaptability.
- Acceleration and torque sensors that monitor rider input and road conditions, allowing real-time adjustments to motor output for a natural and responsive riding experience.
- A static converter that regulates and optimizes the power flow between the battery, motor, and controller, ensuring efficient energy distribution.
- A controller that acts as the system's intelligence hub, processing data from the sensors and executing the embedded control algorithm to manage speed synchronization, power distribution, and dynamic assistance levels.

By integrating these components into a cohesive system, the attachment effectively enhances a conventional cycle vehicle with electric assistance while maintaining full modularity and independence from existing e-bike power sources.

2.1.1. Electrical Motors

Electric cycle configurations commonly include either brushed DC motors or brushless DC (BLDC) motors [21–23]. Due to its higher reliability and power density as well as the reduced dimensions, the more popular choice in recent years has been the brushless DC motors or BLDC. These motors produce torque via electromagnetic interaction between stator windings and rotor-mounted permanent magnets. Furthermore, the advantages of a BLDC motor include its simple and durable electromagnetic design, easy control and excellent power-to-weight ratio. However, its drawbacks include the commutation of phase

currents, significant torque ripple, and a delay in reaching the demanded torque at high speeds. Figure 2 showcases the control strategy of a BLDC motor powering a vehicle.

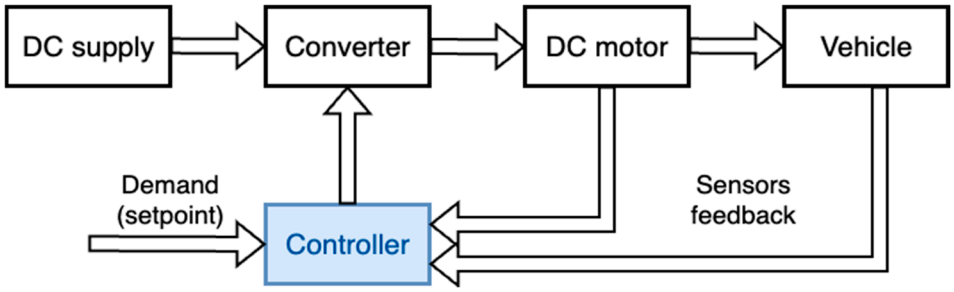


Figure 2. Control scheme for a brushless DC motor (adapted from [24]).

For this demonstrator, the negative effect of the delayed torque response at high rotational speeds is mitigated through the control algorithm. The load-based PID controller running on the STM32 microcontroller (STMicroelectronics, Geneva, Switzerland) is tuned considering the closed-loop dynamics of the motor–controller unit and includes speed-dependent gain adjustment and output filtering, as detailed in Section 3.1. This approach ensures that the attachment can track the required coupling force without inducing oscillations or instability at higher speeds.

The specifications for the DC motors used for the attachment are listed in Table 2.

Table 2. Selected BLDC (model BFSWXK36V250W255R) characteristics (Bafang Electric, Suzhou, China) [25].

Rated Voltage [V]	Rated Power [W]	Rated Current [A]	Efficiency [%]	Weight [kg]	Freewheel Speed [km/h]	Torque [Nm]
36	250	7	≥78%	~3 kg	20–30	20–35

2.1.2. Battery Systems

Battery Energy Storage (BES) is indispensable in the performance of e-bikes, determining key factors such as cost, efficiency, weight, and lifespan [26,27]. The selection of an appropriate battery for e-bikes is influenced by multiple considerations, including energy density, power density, safety, longevity, and affordability [28–32]. Rechargeable batteries used in e-bikes include lithium-ion, lead-acid, nickel-metal hydride (NiMH), vanadium redox, nickel-cadmium (NiCd), zinc-bromine and sodium-sulfur [26,30–32]. Among these, lead-acid batteries are most widely used due to their low cost (approximately $35/kWh) [33]. However, their low energy density makes them heavy compared to modern alternatives. Despite their affordability, they exhibit a short lifespan and low round-trip efficiency, which limits their suitability for high-performance applications.

A key advantage of NiMH batteries is a higher energy density compared to lead-acid batteries while maintaining greater longevity. They are priced at around $350/kWh and, although they exhibit better environmental sustainability and longer cycle life, their relatively lower power density and weight efficiency limit their widespread use in modern e-bikes [33].

Lithium-ion (Li-ion) batteries are the predominant choice in the e-bike market, offering superior energy and power density (200–400 W/L and 500–2000 W/L, respectively), lightweight design, and long service life (5–15 years) [26,33]. Despite their higher price per unit of energy compared to lead-acid batteries (up to 20 times higher) ongoing advancements in manufacturing, such as those from Tesla Motors and Panasonic, have helped lower prices from ~$700/kWh to as low as $300/kWh, with targets near $100/kWh [28].

However, lithium-ion batteries still face notable drawbacks, including high costs and faster discharge rates compared to other types. Despite this, their advantages make them the preferred choice for major e-bike manufacturers [26].

Currently, 70% of Li-ion battery production costs come from the acquisition of raw materials [34]. In this regard, the energy storage system accounts for approximately 30% of an e-bike's total weight (2.0–3.5 kg) and 48% of its total cost [35]. The placement of the battery pack influences ride comfort, with studies suggesting (based on weighted vertical acceleration analysis [36]) that mounting the battery under the seat tube offers better comfort compared to rear cargo rack placement [36]. Other rechargeable options, such as vanadium redox flow batteries (VRBs), offer higher round-trip efficiency, longer discharge durations, and extended service life. However, due to their complex structure and high cost, they are less commonly used in commercial e-bike applications [26].

Ongoing advancements in battery technology, manufacturing efficiency, and material sourcing are expected to further reduce costs and improve overall battery performance, ensuring continued innovation in the e-bike industry [26]. The specifications for the batteries used for the attachment are listed in Table 3.

Table 3. Selected battery (model YJ1281005) characteristics (YJ Power Group Limited, Shenzhen, China) [37].

Nominal Voltage [V]	Rated Capacity [Ah]	Rated Energy [Wh]	Weight [kg]
36	16	576	3.11

2.1.3. Sensors and Controllers

E-bikes rely on various sensors to optimize their performance. These sensors play a crucial role in monitoring the rider's input and the vehicle's conditions, enabling real-time adjustments to power delivery. Among the most commonly used sensors are torque sensors, which measure the force applied by the cyclist; cadence sensors, which track the pedal rotation speed; and speed sensors, which monitor the vehicle's velocity. The data collected from these sensors allows the motor controller to regulate power output efficiently, ensuring smooth and intuitive assistance [38].

Modern PEDELECs in Europe primarily operate using a powertrain controller with a "constant gain" strategy. This control logic is based on three key parameters: the cyclist's torque input, cadence, and vehicle speed. Riders may choose among three to five operating modes to set their preferred assistance level, with the exact options varying by manufacturer and e-bike model. To comply with EU regulations, e-bikes are subject to a speed limit of 25 km/h. Once this threshold is reached, the motor controller automatically disables assistance, ensuring that the vehicle does not exceed legal speed constraints while maintaining a natural pedaling experience [28].

E-Bikes with embedded intelligence remain in the early stages of development [39]. Many e-Bike brands market their offerings as "intelligent", often as a promotional strategy rather than a reflection of true advanced functionality. Some models incorporate onboard computing systems equipped with Global Positioning System (GPS), anti-theft tracking, and connectivity options with smartphones via Bluetooth and Universal Serial Bus (USB) [28]. Other e-Bike models allow users to connect their smartphones, leveraging built-in GPS and sensors to analyze and display ride-related data or share it on social networks [40]. These features typically support navigation, performance tracking, and health monitoring. Furthermore, recent innovations include interactive feedback on handlebars, such as flashing lights and vibration alerts, as seen in the crowdsourced e-Bike by Canadian company Vanhawks Valour (Toronto, Canada). This system helps cyclists navigate routes with minimal distractions, improving road safety by alerting riders to hazards ahead [41].

Additionally, modern intelligent e-Bikes claim to provide users with detailed ride data, including bike location (longitude, latitude, altitude, and time), motor assistance usage, and sensor-based metrics such as seating pressure and foot pressure distribution. However, despite collecting this information, many systems fail to offer clear insights into how these data points benefit users or enhance the riding experience [28,42]. The specifications for the controllers used for the attachment are listed in Table 4.

Table 4. Selected controller (model LSW943-92F) characteristics (Nanjing Lishui Electronics Research Institute Co., Ltd., Nanjing, China) [43].

Rated Voltage [V]	Maximum Current [A]	Rated Current [A]	Low Voltage Protection [V]	Throttle Adjustment Voltage [V]
36	14	7	31.5	1.2–4.4

In terms of controllers, the main input given by the driver is the throttle signal which is processed and regulates the motor through the motor driver. The motor voltage is adjusted according to throttle values, allowing precise control over power and speed. Additionally, the controller continuously monitors speed sensor readings. The speed sensor operates based on the Hall effect principle, transmitting real-time wheel RPM data [44]. Some controllers are designed solely for basic operations such as acceleration and pedal-assist control, while more advanced controllers offer greater processing power. These advanced controllers can manage multiple features using various inputs, outputs, and complex algorithms [45].

In ref. [46], an integrated powertrain control system is introduced, based on proportional-integral-derivative (PID) control. The system utilizes a BLDC hub motor, which is managed through field-oriented control for both driving and braking operations. Simulation results using a DC motor are presented in ref. [47]. In ref. [48], an ATMEGA-32 microcontroller is employed to regulate the analog input from the throttle in an e-bike. A similar approach is described in ref. [49], where an Arduino-based control drive is implemented for a brushless DC hub motor. Further simulations and a comprehensive system description are provided in ref. [50].

Although multiple microcontroller options are available for e-bike applications the STM32 microcontrollers offer distinct advantages, including real-time communication with other system components. STM32CubeIDE (STMicroelectronics, version 1.16.1) provides an integrated environment for coding, debugging, and peripheral configuration, making it highly suitable for firmware development. When applied to e-bike control systems, STM32 platforms support customized software implementations that refine speed-control algorithms and user interfaces, resulting in reliable speed regulation and enhanced user interaction [44].

The development board used for the demonstrator is the STM32 NUCLEOF030R8 board (STMicroelectronics, Geneva, Switzerland) having the following purposes:

- Managing the data acquisition from the two load cells;
- Sending data over serial through the UART protocol for logging, display and debugging;
- Processing the sensor values and executing the PID control algorithm to generate the throttle signals.

The two CZL635 single-point load cells (Guangdong South China Sea Electronic Measuring Technology Co., Ltd.: Guangdong, China) were selected for their high precision (0.05% FS), compact form factor, and suitability for low-capacity force measurements up to 20 kg, ensuring accurate detection of coupling forces within the experimental setup [51]. The specifications for the HX711 modules (Avia Semiconductor, Xiamen, China) used for the attachment are listed in Table 5.

Table 5. CZL635 load cell characteristics [51].

Capacity [kg]	Precision [%]	Rated Output [mv/V]	Excitation Voltage [V]
20	0.05	1.0 ± 0.15 mv/V	5

Two HX711 modules were used to amplify the signal coming from the load cells and to convert the incoming signal from analogue to digital format. The specifications for the HX711 modules used for the attachment are listed in Table 6.

Table 6. HX711 module characteristics [52].

Power Supply Voltage [V]	Analog Supply Current [μA]	Digital Supply Current [μA]	Output Settling Time [ms]	Reference Bypass [V]
2.6–5.5	1400	100	400	1.25

3. Software

3.1. Speed Control Loop

The control strategy for the demonstrator is shown in Figure 3. The two load cells are mounted on the attachment's coupling mechanism to the leading vehicle. Each load cell reading is used as feedback in the PID controller and generates the setpoint for the DC motor to keep the force applied on the cell as close to zero as possible.

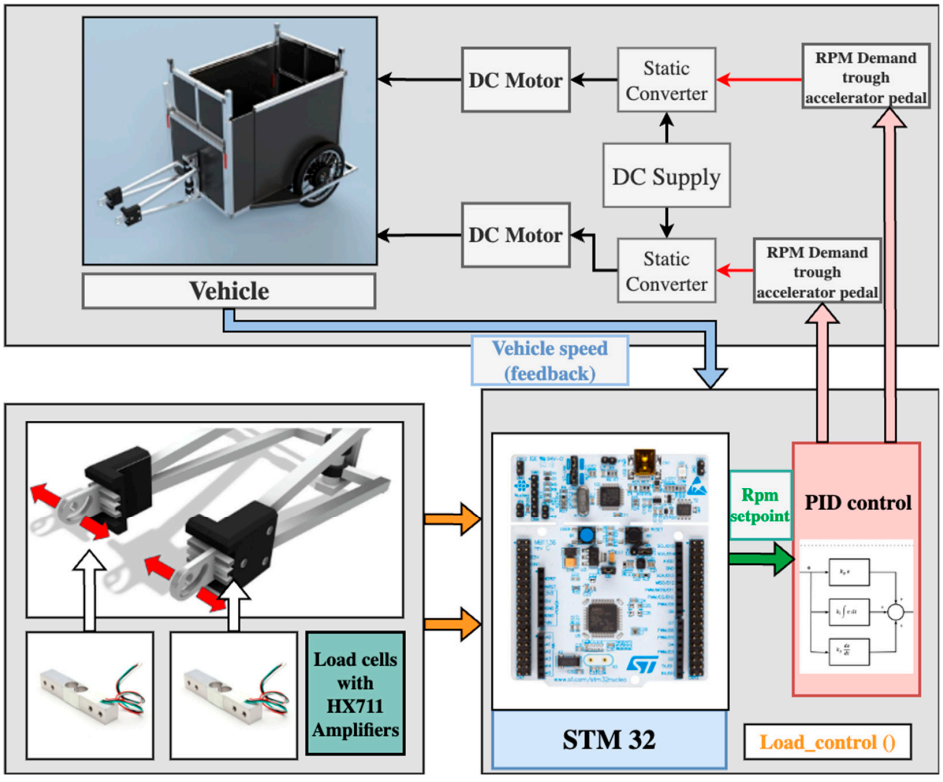


Figure 3. Control strategy for the electrical assistance system of the attachment.

As long as the value is higher than zero, it means that the leading vehicle is pulling the attachment forward, which creates additional effort for the driver. This can be adjusted by increasing the motor's speed. On the other side, if the values are negative, it means that the attachment is pushing the vehicle, which can cause instability for the overall system both in maintaining a certain speed and keeping a straight trajectory. In Figure 4, four movement cases are shown to illustrate the different combinations of positive and negative load cell readings depending on the action of the leading cycle. Figure 4a shows linear forward

movement. In this case a positive load value can be expected on both sensors, causing the attachment to accelerate until the leading vehicle's velocity is reached. Conversely Figure 4b shows the reverse situation where the leading vehicle either moves backwards or brakes. In this case negative load values can be expected from both sensors, causing the attachment to reduce its speed until equilibrium is achieved. Two non-linear movement cases are displayed in Figure 4c,d. In both scenarios, the two sensors register different load polarity values, requiring the controller to adjust each motor's speed independently.

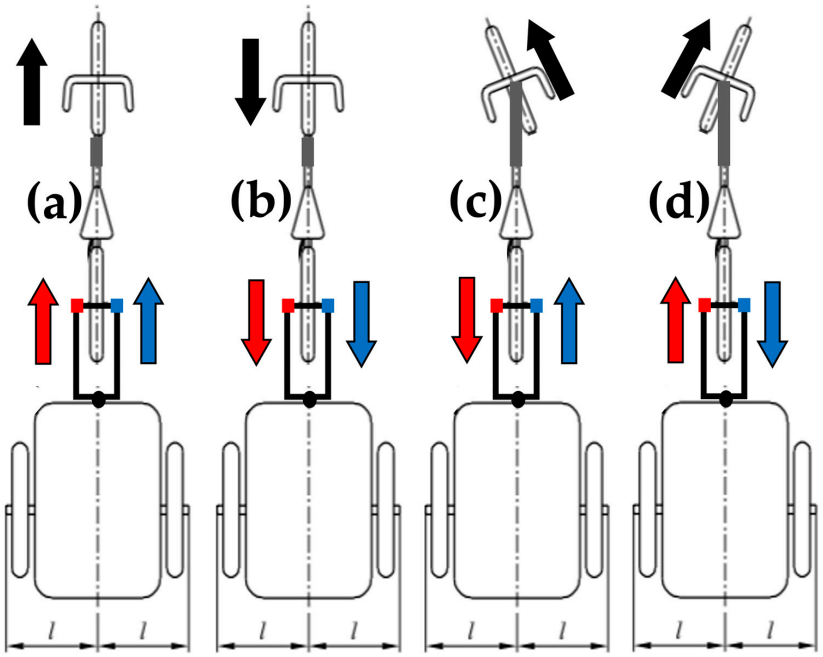


Figure 4. Load readings in the coupling assembly in different moving scenarios for the attachment-cycle system. (**a**) linear movement forward; (**b**) leading cycle braking; (**c**) left turn; (**d**) right turn.

Using the selected hardware components, a prototype of the sensors–controller assembly was built to test the software component responsible for controlling the trailer's electric motors. The system evaluates the commands sent by the STM32 control unit to the actuators under different forces acting on the coupling system between the trailer and the leading vehicle, as measured by the load cells. Both the signal simulating the forces applied to the coupling mechanism and the calculated motor control signal are displayed through a simple Python (Python Software Foundation, version 3.12) application, developed for the purpose of validating the controller's functionality.

The controller outputs two DC motor setpoints and receives feedback in the form of two signals through the loads measured on the attachment coupling mechanism. This allows the attachment to steer due to the fact that the command for one DC motor is calculated based on the load signal from the load cell on the same side. To exemplify this scenario the following sensor readings are considered in Figure 5: a negative load value on the left-side sensor and a positive load value on the right one. This would mean that there is a negative force applied on the left side of the coupling mechanism (the attachment pushing the leading vehicle) and a positive force on the opposite side (the leading vehicle dragging the attachment). This translates to a left turn initiated by the driver. Because both controllers have to keep the sensor value readings as close to 0 as possible, the command given to the left-side motor will decrease its RPM and an acceleration command will be given to the right-side motor. Conversely, a right-turn scenario would exhibit inverted load values on the two sensors, producing opposite motor responses.

The PID_Compute() function implements a discrete PID controller that continuously adjusts the PWM output based on the error between the desired setpoint (0 load value) and the current load cell reading.

```
// Variable definition
float Maximum_rate = 15f;              // Max change of output per cycle
float Previous_Output_value = 0.0f;  // Last throttle value
// PID Parameters
float setpoint = 0.0f;                 // Desired force = 0
float Kp_low = 0.8f;                   // Proportional gain low speed region
float Kp_high = 0.4f;                  // Proportional gain near maximum speed
float Ki = 0.05f;                      // Integral gain
float Kd = 0.3f;                       // Derivative gain
// Threshold for adaptive control
float Motor_Command_threshold = 80.0f;
// Integral limits for anti-windup
#define INTEGRAL_MAX 200.0f
#define INTEGRAL_MIN -200.0f
// PID State variables
float integral = 0.0f;
float previous_error = 0.0f;
```

```
// PID Controller Function
uint32_t PID_Compute(float input)
{
    float error = setpoint-input;
    // Adaptive Kp
    float Kp = (Previous_Output_value < Motor_Command_threshold) ? Kp_low : Kp_high;
    // Derivative calculation
    float derivative = error-previous_error;
    previous_error = error;
    // Output calculation before integral update
    float output = Kp * error + Ki * integral + Kd * derivative;
    // Rate limiting
    if (output > Previous_Output_value + Maximum_rate)
        output = Previous_Output_value + Maximum_rate;
    if (output < Previous_Output_value - Maximum_rate)
        output = Previous_Output_value - Maximum_rate;
    // Output saturation
    if (output < 0) output = 0;
    if (output > 100) output = 100;
    if (!((output <= 0 && error < 0) || (output >= 100 && error > 0))) {
        integral += error;
        // Clamp integral to prevent excessive accumulation
        if (integral > INTEGRAL_MAX) integral = INTEGRAL_MAX;
        if (integral < INTEGRAL_MIN) integral = INTEGRAL_MIN;
    }
    Previous_Output_value = output;
    return (uint32_t)output;
}
```

The function calculates a proportional term (reacting to the current error), an integral term (accumulating past errors to correct steady-state drift), and a derivative term (predicting future error trends to dampen oscillations). These terms are combined and scaled by Kp_high, Kp_low, Ki, and Kd, respectively, to produce a control output, which is then saturated between 0 and 100 and used to set the motor's PWM duty cycle, helping maintain balance around the target force applied by the leading cycle vehicle.

To address the limitations of BLDC hub motors at higher rotational speeds, the PID controller was extended with adaptive gain scheduling and output rate limiting. Combining these measures ensures an improved closed-loop behavior at different operation points. The adaptive proportional gain is employed because the torque response of a BLDC motor decreases as it reaches the electromotive-force–limited operating region. Using a fixed proportional gain (Kp) can lead to oscillatory behavior when the motor command approaches its upper range. To overcome this, the controller monitors the previous throttle output and switches between two proportional gains. When the motor command is below a defined threshold (80% of maximum), the controller uses a higher Kp for rapid force correction. When the command exceeds this threshold, a reduced Kp is applied to prevent aggressive corrections.

In addition to adaptive gains, a rate limiter was introduced to constrain the maximum allowed change in the throttle signal between consecutive control cycles. This ensures that, even if the calculated error momentarily increases, the controller will not request torque steps that exceed the motor's achievable torque slew rate. At higher command levels the rate limiter synchronizes the commanded torque changes, eliminating the risk of opposite sign oscillations in the hitch. To maintain stability during prolonged saturation or when the load force is close to zero, integral action is updated only when the output is within its valid range. Additionally, the integral term is clamped to predefined limits. This prevents integral windup and ensures predictable behavior under rapidly changing load conditions.

To preliminarily assess the behavior of the proposed controller independently of the mechanical attachment, an open-loop simulation was performed on the PID controller. The controller was excited with a representative force profile designed to stress the adaptive gain, rate limiter, and anti-windup mechanisms. The resulting performance metrics demonstrate that the controller reacts consistently and remains numerically stable across the full operating range (Table 7).

Table 7. Performance metrics of the PID controller.

Parameter	Value
Time in Deadband	3.00 s
Settling Time	3.49 s
Integral of Absolute Error	703.24
Integral of Squared Error	33,187.25
Integral of Time-weighted Absolute Error	6459.90
Rise Time	0.39 s

For the purpose of this preliminary assessment, the simulated sensor signal was chosen to simulate a real urban scenario with hitch forces reflective of starting, braking as well as induced oscillations that could occur. The input dataset reflects sensor readings equivalent to a range between 60 N and −50 N which translates to a low cargo load in the attachment's compact configuration. The simulated hitch force as well as the output calculated by the controller are shown in Figure 6.

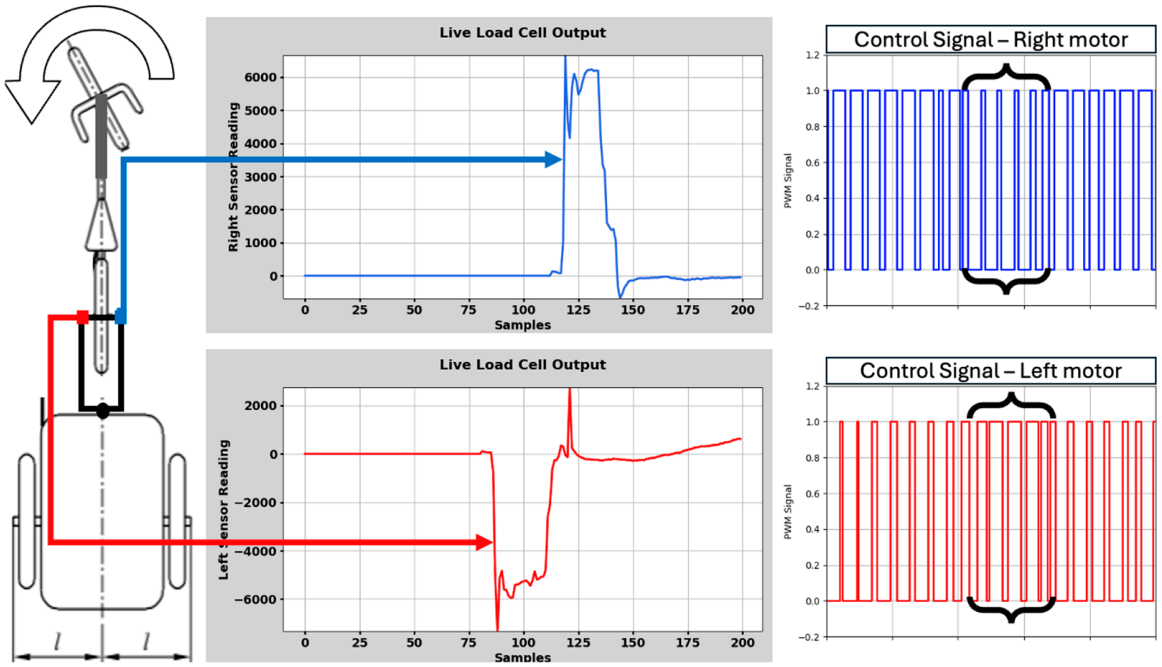


Figure 5. Control strategy in the case of a left turn.

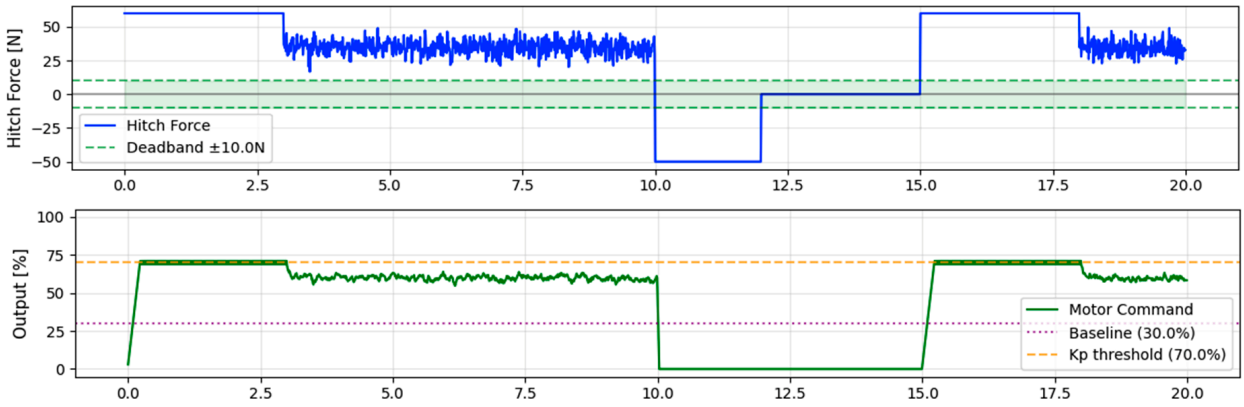


Figure 6. Simulated hitch force and calculated motor command in an open loop test.

The parameters used in the presented simulation constitute an initial tuning chosen to ensure numerical stability and safe control action during early development. The PID controller will undergo systematic retuning using in closed loop to allow the final controller to be optimized for stability, responsiveness, and safety under real operating conditions.

3.2. Data Visualization in Python

In the process of developing the algorithm for the electrical assistance system, a simple tool for data visualization was created using python to check the UART connection of the STM32 by analyzing incoming sensor readings while also allowing different configurations for displaying the results.

```
SERIAL_PORT = "COM8"
BAUD_RATE = 115200
ser = serial.Serial(SERIAL_PORT, BAUD_RATE, timeout=1)
BUFFER_SIZE = 100
data = deque([0] * BUFFER_SIZE, maxlen=BUFFER_SIZE)
plt.ion()
fig, ax = plt.subplots()
line, = ax.plot(data)
while True:
    try:
        line_data = ser.readline().decode(errors='ignore').strip()
        if "Load1" in line_data:
            data.append(line_data)
            line.set_ydata(data)
            ax.set_ylim(min(data)-10, max(data)+10)
    except ValueError:
        print(f"Skipping: {line_data}")
ser.close()
plt.ioff()
plt.show()
```

This Python script enables a serial connection with an STM32 microcontroller to receive and visualize real-time data for the load cell module. It is configured to read from a specified COM port (COM8) at a baud rate of 115,200 and continuously reads incoming serial data. The script filters for lines containing the label "Load1" to extract sensor measurements, which are expected in a numerical format (e.g., "Load1: 1234 g"). These values are parsed, appended to a fixed-length buffer (using a deque with a size of 100), and plotted live using the matplotlib library. The plot dynamically updates with each new reading, including auto-scaling the Y-axis based on incoming data. It also includes error handling for malformed data and allows clean termination through a keyboard interrupt.

4. Serial Communication

In order to ensure the attachment's electrical assistance function, reliable data acquisition was paramount both for testing, validating and optimizing the implemented controller. For this reason, the prototype was developed for the purpose of data acquisition and debugging, so all the signals can be plotted and recorded. The development process began with configuring an STM32CubeIDE project for the NUCLEO-F030R8 board, integrating HX711 load cell amplifiers for force measurement. The final configurations for the internal clock are visible in Table 8.

Table 8. Internal clock configuration.

Parameter	Value
Internal High-Speed Oscillator (HSI)	8 MHz
Input to PLL: HSI/2	4 MHz
PLL Multiplier	×12
PLL Output	4 MHz × 12 = 48 MHz
System Clock (SYSCLK)	PLLCLK
Frequency	48 MHz
AHB Prescaler	HCLK = 48 MHz
APB1 Prescaler	PCLK1 = 48 MHz
USART Clock: Derived from PCLK1	48 MHz
UART baud rate	115,200

Initial tests focused on reliably acquiring and transmitting sensor data via UART, validated through STM32CubeMonitor (STMicroelectronics, version 1.10.0). Various methods were explored to optimize the data transmission rate, including reducing message length, increasing the UART baud rate, and switching from text-based to binary data formats. A custom data frame with defined start and end markers was implemented to ensure data integrity and efficient parsing. These enhancements were tested and confirmed using both a real-time Python visualization script and the STM32CubeMonitor application. Figure 7 shows a test performed to check the responsiveness of the sensor to static conditions with a static force applied to the center of the load cell.



Figure 7. Load cell data transmission test via UART.

5. Discussion

The proposed electrically assisted modular attachment represents a sustainable modular solution for urban services having increased transport capacity, enhanced trip efficiency through its variable cargo volume and being compatible with a wide range of cycle vehicles. Its independence from the leading vehicle's electrical system makes it a versatile and transferable solution for urban logistics, while the modular design supports flexible use in diverse delivery scenarios. However, limitations remain, such as potential challenges related to battery autonomy and durability under intensive use. From a production perspective, the use of widely available e-bike components supports cost-effective manufacturing and maintenance, yet scaling up requires standardization of the coupling mechanism and further validation of safety compliance. Large-scale implementation could be enabled by partnerships with logistics providers and urban mobility programs, while future development should focus on refining the control algorithm, improving energy efficiency, and integrating connectivity features for fleet management. Further planned activities that will provide data regarding public acceptance and collaborations include surveys for local logistics companies, feasibility study and SWOT analysis with cost impact.

6. Conclusions

This study presents the development of an electrical assistance system for a modular cargo attachment designed for lightweight cycles used in urban parcel transportation. By leveraging widely available e-bike technologies such as BLDC motors, lithium-ion battery systems, torque and speed sensors, and embedded microcontrollers, this solution demonstrates the potential to convert conventional cycle vehicles into efficient, e-powered logistics vehicles. The modular aspect of the system addresses a critical limitation in current cargo cycles design: lack of adaptability in terms of coupling and cargo volume. This may discourage users from adopting micromobility solutions particularly at the entry level, where cargo cycle options remain limited. The variable cargo volume ensures the maximum trip efficiency by giving the users the option of adjusting the size of the attachment when needed. Furthermore, with an independent electrical system and real-time adaptive speed control, the attachment maintains optimal performance across varying payloads and urban driving scenarios.

The control algorithm based on dual load-cell feedback and PID control ensures dynamic synchronization with the leading cycle. This strategy minimizes driver effort while avoiding instability due to push–pull dynamics during acceleration, braking, or cornering. Moreover, the integration of accessible firmware tools like STM32CubeIDE and Python-based data monitoring provides an open and scalable development pathway, ensuring that further enhancements in control precision and user feedback are viable.

This effort contributes to the advancement of sustainable urban mobility by offering a zero-emission, space-efficient, and cost-effective alternative to traditional last-mile delivery vehicles such as vans and trucks. Given the increasing demand for urban environments to prioritize the decarbonization process in the transport sector and reduce congestion, modular solutions can play a key role in micromobility ecosystems. Additionally, by allowing compatibility with a wide range of pedal vehicles, multiple users can share the attachment for on-demand scenarios.

Future work will focus on refining the control algorithm and testing the system in different scenarios. Pilot programs in real-world logistics operations will also be necessary to evaluate the long-term durability, user acceptance, and operational savings of the system. As cities increasingly prioritize climate neutrality and active mobility, innovations are essential in shaping the future of urban freight transport.

Author Contributions: Conceptualization, N.V.B. and V.T.; investigation, I.C.S.; software and visualization V.T.; writing—original draft preparation, V.T.; writing—review and editing, I.D., A.M., L.B.K. and N.B.; supervision, N.B.; project administration, L.B.K.; funding acquisition, L.B.K. All authors have read and agreed to the published version of the manuscript.

Funding: This work was supported by the Technical University of Cluj Napoca under the GNaC ARUT 2023 National Grant Program, grant number 25/01-07-2024.

Data Availability Statement: The original contributions presented in this study are included in the article. Further inquiries can be directed to the corresponding author.

Conflicts of Interest: The authors declare no conflicts of interest.

Abbreviations

The following abbreviations are used in this manuscript:

BLDC	Brushless Direct Current (Motor)
BES	Battery Energy Storage
DC	Direct Current
PID	Proportional–Integral–Derivative (Controller)

PEDELEC	Pedal Electric Cycle
GPS	Global Positioning System
USB	Universal Serial Bus
UART	Universal Asynchronous Receiver-Transmitter
STM32	STMicroelectronics 32-bit Microcontroller
IDE	Integrated Development Environment
COM Port	Communication Port
RPM	Revolutions Per Minute
HSI	High-Speed Internal (Oscillator)
PLL	Phase-Locked Loop
SYSCLK	System Clock
SWOT	Strengths, Weaknesses, Opportunities, Threats

References

1. European Commission. Sustainable and Smart Mobility Strategy-Putting European Transport on Track for the Future. 2020. Available online: https://eur-lex.europa.eu/legal-content/EN/TXT/?uri=CELEX%3A52020DC0789 (accessed on 30 June 2025).
2. Dornoff, J.; Mock, P.; Baldino, C.; Bieker, G.; Díaz, S.; Miller, J.; Sen, A.; Tietge, U.; Wappelhorst, S. Fit for 55: A Review and Evaluation of the European Commission Proposal for Amending the CO_2 Targets for New Cars and Vans. 2021. Available online: https://theicct.org/sites/default/files/publications/fit-for-55-review-eu-sept21.pdf (accessed on 16 November 2025).
3. CityChangerCargoBike Project Consortium. CityChangerCargoBike: Increasing the Take-Up and Scale-Up of Cargo Bikes in Urban Areas; Grant Agreement 769086; H2020 Programme; European Commission: Brussels, Belgium, 2018–2022. Available online: https://cordis.europa.eu/project/id/769086 (accessed on 16 November 2025).
4. Urban Logistics as an on Demand Service Project Consortium. Urban Logistics as an on Demand Service: Sustainable System Innovations in Urban Logistics; Grant Agreement 861833; H2020 Programme; European Commission: Brussels, Belgium, 2020–2024. Available online: https://cordis.europa.eu/project/id/861833 (accessed on 16 November 2025).
5. Dorsey, B. Sustainable Intermediate Transport in West Africa: Quality Before Quantity. *World Transp. Policy Pract.* **2008**, *14*, 8–20.
6. Lenz, B.; Riehle, E. Bikes for Urban Freight? *Transp. Res. Rec. J. Transp. Res. Board* **2013**, *2379*, 39–45. [CrossRef]
7. Schier, M.; Offermann, B.; Weigl, J.D.; Maag, T.; Mayer, B.; Rudolph, C. Innovative two wheeler technologies for future mobility concepts. In Proceedings of the 2016 11th International Conference on Ecological Vehicles and Renewable Energies, EVER 2016, Monte Carlo, Monaco, 6–8 April 2016. [CrossRef]
8. Oyesiku, O.O.; Akinyemi, O.O.; Giwa, S.O.; Lawal, N.S.; Adetifa, B.O. Evaluation of Rural Transportation Technology: A Case Study of Bicycle and Motorcycle Trailers. *J. Kejuruter.* **2019**, *31*, 11–18. [CrossRef]
9. NÜWIEL. NÜWIEL eTrailer. Available online: https://www.nuwiel.com (accessed on 24 June 2025).
10. Aevon. CARGO 10. Available online: https://aevon-trailers.com/en/homepage/ (accessed on 16 November 2025).
11. Carla Cargo. e-Carla Cargo. Available online: https://www.carlacargo.de/products/ecarla (accessed on 24 June 2025).
12. Teodorascu, V.; Burnete, N.; Kocsis, L.B.; Duma, I.; Molea, A.; Sechel, I.C. Design and validation of an electrically assisted modular attachment demonstrator for lightweight cycles. *J. Eng. Sci. Innov.* **2024**, *9*, 431–448. [CrossRef]
13. Burley. Travoy® Cargo Trailer. Available online: https://burley.com/en-in/products/travoy (accessed on 16 November 2025).
14. Burley. Flatbed™ Cargo Trailer. Available online: https://burley.com/en-in/products/flatbed (accessed on 16 November 2025).
15. TAXXI. LOAD Heavy—Trailer for Heavy Loads and Luggage. Available online: https://mytaxxi.de/en/products/taxxi-load-heavy (accessed on 16 November 2025).
16. Wike. Aluminum Landscaping & Utility Cargo Bike Trailer. Available online: https://wikeinc.com/en-ca/products/cargo-landscaping-trailer (accessed on 16 November 2025).
17. *ASTM F2917-12*; Standard Specification for Bicycle Trailer Cycles Designed for Human Passengers. ASTM International: West Conshohocken, PA, USA, 2012. [CrossRef]
18. *ASTM F1975-09*; Standard Specification for Nonpowered Bicycle Trailers Designed for Human Passengers. ASTM International: West Conshohocken, PA, USA, 2015. [CrossRef]
19. *BS EN 15918:2011*; Cycles—Cycle Trailer—Safety Requirements and Test Methods. SGS: Baar, Switzerland, 2011. Available online: https://knowledge.bsigroup.com/products/cycles-cycle-trailers-safety-requirements-and-test-methods (accessed on 16 November 2025).
20. Gov. of Romania. DECISION No. 1,391 of October 4, 2006, for the Approval of the Regulation for the Implementation of Government Emergency Ordinance No. 195/2002 Regarding Traffic on Public Roads. Available online: https://legislatie.just.ro/Public/DetaliiDocument/164781 (accessed on 16 November 2025).
21. Muetze, A.; Tan, Y.C. Electric bicycles—A performance evaluation. *IEEE Ind. Appl. Mag.* **2007**, *13*, 12–21. [CrossRef]

22. Starschich, E.; Muetze, A. Comparison of the performances of different geared brushless-DC motor drives for electric bicycles. In Proceedings of the IEEE International Electric Machines and Drives Conference, IEMDC 2007, Antalya, Turkey, 3–5 May 2007; Volume 1, pp. 140–147. [CrossRef]
23. Adnan, A.; Ishak, D. Finite element modeling and analysis of external rotor brushless DC motor for electric bicycle. In Proceedings of the 2009 IEEE Student Conference on Research and Development—SCOReD 2009, Serdang, Malaysia, 16–18 November 2009; pp. 376–379. [CrossRef]
24. Contò, C.; Bianchi, N. E-Bike Motor Drive: A Review of Configurations and Capabilities. *Energies* **2023**, *16*, 160. [CrossRef]
25. Bafang Electric (Suzhou) Co., Ltd. BFSWXK36V250W255R Brushless Hub Motor Specifications; Bafang Electric: Suzhou, China. Available online: https://www.bafang-e.com/en/oem-area/components/motor/ (accessed on 16 November 2025).
26. Arsadiando, W.; Sutikno, T.; Widodo, N.S.; Santosa, B. Comprehensive Analysis of Current Research Trends in Battery Technologies as Electricity Storage Devices for Electric Bikes: A Review. *JEEE* **2022**, *15*, 138–143. Available online: https://www.researchgate.net/publication/376810202 (accessed on 16 November 2025).
27. Weinert, J.X.; Burke, A.F.; Wei, X. Lead-acid and lithium-ion batteries for the Chinese electric bike market and implications on future technology advancement. *J. Power Sources* **2007**, *172*, 938–945. [CrossRef]
28. Stilo, L.; Segura-Velandia, D.; Lugo, H.; Conway, P.P.; West, A.A. Electric bicycles, next generation low carbon transport systems: A survey. *Transp. Res. Interdiscip. Perspect.* **2021**, *10*, 100347. [CrossRef]
29. Such, M.C.; Hill, C. Battery energy storage and wind energy integrated into the smart grid. In Proceedings of the 2012 IEEE PES Innovative Smart Grid Technologies, ISGT 2012, Washington, DC, USA, 16–20 January 2012. [CrossRef]
30. Bhatt, J.M.; Ramana, P.V.; Mehta, J.R. Performance assessment of valve regulated lead acid battery for E–bike in field test. *Mater. Today Proc.* **2022**, *49*, 2058–2065. [CrossRef]
31. Fishman, E.; Cherry, C. E-bikes in the Mainstream: Reviewing a Decade of Research. *Transp. Rev.* **2016**, *36*, 72–91. [CrossRef]
32. Hannan, M.A.; Hoque, M.M.; Mohamed, A.; Ayob, A. Review of energy storage systems for electric vehicle applications: Issues and challenges. *Renew. Sustain. Energy Rev.* **2017**, *69*, 771–789. [CrossRef]
33. Hung, N.B.; Lim, O. A review of history, development, design and research of electric bicycles. *Appl. Energy* **2020**, *260*, 114323. [CrossRef]
34. Fogel, D. *Strategic Sustainability: A Natural Environmental Lens on Organizations and Management*; Taylor & Francis Group: Boca Raton, FL, USA, 2016; pp. 1–354. [CrossRef]
35. Kerdsup, B.; Fuengwarodsakul, N.H. Performance and cost comparison of reluctance motors used for electric bicycles. *Electr. Eng.* **2017**, *99*, 475–486. [CrossRef]
36. Du, W.; Zhang, D.; Zhao, X. Research on battery to ride comfort of electric bicycle based on multi-body dynamics theory. In Proceedings of the 2009 IEEE International Conference on Automation and Logistics, ICAL 2009, Shenyang, China, 5–7 August 2009; pp. 1722–1726. [CrossRef]
37. YJ Power Group Limited (Shenzhen), Shenzhen, China. Model YJ1281005 Electric Bicycle Battery (36V, 16Ah, 576Wh). Available online: https://www.jetechbattery.com/products (accessed on 16 November 2025).
38. Khanke, P.K.; Jain, S.D. Comparative analysis of speed control of BLDC motor using PI, simple FLC and Fuzzy-PI controller. In Proceedings of the International Conference on Energy Systems and Applications, ICESA 2015, Pune, India, 30 October–1 November 2015; IEEE: New York, NY, USA, 2016; pp. 296–301. [CrossRef]
39. About the Smart Ebike Project—E Mountain Bikes. Available online: https://emountainbikekings.com/events/smart-ebikes/ (accessed on 16 November 2025).
40. Robert Bosch GmbH. Bosch eBike Systems. Available online: https://www.bosch-ebike.com/en/ (accessed on 16 November 2025).
41. Zahid, A. Vanhawks Valour | First Ever Connected Carbon Fibre Bicycle. Available online: https://www.kickstarter.com/projects/1931822269/vanhawks-valour-first-ever-connected-carbon-fibre (accessed on 16 November 2025).
42. Kiefer, C.; Behrendt, F. Smart e-bike monitoring system: Real-time open source and open hardware GPS assistance and sensor data for electrically assisted bicycles. *IET Intell. Transp. Syst.* **2016**, *10*, 79–88. [CrossRef]
43. Nanjing Lishui Electronics Research Institute Co., Ltd. LSW943-92F Brushless Motor Controller for Electric Bicycles; Lishui Controller: Nanjing, China. Available online: https://www.lsdzs.com/ls_product/product.php?lang=en&class2=19 (accessed on 16 November 2025).
44. Tamilmani, T.; Tanushri, K. E-Bike Speed Control System. *JETIR* **2023**, *10*, b864–b871. Available online: https://www.jetir.org/view?paper=JETIR2312206 (accessed on 16 November 2025).
45. Thakare, C.S. A Review Paper on-E-Bike Motor Speed Controller. *Int. J. Adv. Res. Sci. Commun. Technol. IJARSCT* **2023**, *3*, 314–317. [CrossRef]
46. Lin, C.L.; Chen, E.P.; Chen, Y.C.; Liu, M.K. Advanced driving/braking control design for electric bikes. In Proceedings of the 2017 12th IEEE Conference on Industrial Electronics and Applications, ICIEA 2017, Siem Reap, Cambodia, 18–20 June 2017; pp. 1254–1259. [CrossRef]

47. Kaushik, M.V.S. Model based design to control DC motor for pedal assist bicycle. In Proceedings of the 2015 IEEE International Conference on Electrical, Computer and Communication Technologies, ICECCT 2015, Coimbatore, India, 5–7 March 2015. [CrossRef]
48. Mohan, S.; Jayasree, P.R.; Ravi, S.; Prasad, R.; Vijayakumar, V. Economically viable conversion of a pedal powered bicycle into an electric bike. In Proceedings of the 2013 International Conference on Electrical Machines and Systems, ICEMS 2013, Busan, Republic of Korea, 26–29 October 2013; pp. 450–453. [CrossRef]
49. Faruque, K.F.I.; Nawshin, N.; Bhuiyan, M.F.; Uddin, M.R.; Hasan, M.; Salim, K.M. Design and Development of BLDC Controller and Its Implementation on E-Bike. In Proceedings of the 2018 International Conference on Recent Innovations in Electrical, Electronics and Communication Engineering, ICRIEECE 2018, Bhubaneswar, India, 27–28 July 2018; pp. 1461–1465. [CrossRef]
50. Thejasree, G.; Maniyeri, R.; Kulkami, P. Modeling and Simulation of a Pedelec. In Proceedings of the 2019 Innovations in Power and Advanced Computing Technologies, i-PACT 2019, Vellore, India, 22–23 March 2019. [CrossRef]
51. Guangdong South China Sea Electronic Measuring Technology Co., Ltd.: Guangdong, China. 3134-Micro Load Cell (0–20 kg)-CZL635. Available online: http://www.mantech.co.za/datasheets/products/CZL635-EIE.pdf (accessed on 16 November 2025).
52. Avia Semiconductor. HX711: 24-Bit Analog-to-Digital Converter (ADC) for Weigh Scales. HX711 Datasheet (Rev. English). Available online: https://cdn.sparkfun.com/datasheets/Sensors/ForceFlex/hx711_english.pdf (accessed on 19 August 2025).

Disclaimer/Publisher's Note: The statements, opinions and data contained in all publications are solely those of the individual author(s) and contributor(s) and not of MDPI and/or the editor(s). MDPI and/or the editor(s) disclaim responsibility for any injury to people or property resulting from any ideas, methods, instructions or products referred to in the content.